

# Highly effective hybrid catalyst for the direct synthesis of dimethyl ether from syngas with magnesium oxide-modified HZSM-5 as a dehydration component

Dongsen Mao\*, Weimin Yang, Jianchao Xia, Bin Zhang, Qingying Song, Qingling Chen

Shanghai Research Institute of Petrochemical Technology, SINOPEC, Shanghai 201208, P.R. China

## Abstract

A series of HZSM-5 zeolites modified with various contents of magnesium oxide (0–10 wt%) were prepared with an incipient impregnation technique and characterized by X-ray diffraction, N<sub>2</sub> adsorption, temperature-programmed desorption of NH<sub>3</sub> and CO<sub>2</sub>, <sup>27</sup>Al MAS NMR, and FT-IR. The modified HZSM-5 zeolites were mixed physically with methanol synthesis components (Cu–ZnO–Al<sub>2</sub>O<sub>3</sub>) to perform the direct synthesis of dimethyl ether (DME) from syngas under pressurized fixed-bed continuous-flow conditions. The results indicated that modification of HZSM-5 with a suitable amount of MgO significantly decreased the selectivities for undesired by-products like hydrocarbons and CO<sub>2</sub> from 9.3 and 37.1% to less than 0.4 and 31%, respectively, through the removal of unselective strong Brønsted acid sites and hence enhanced the selectivity for DME from 49% to more than 64%, whereas the conversion of carbon monoxide was scarcely affected. However, when the MgO contents were equal to or higher than 5 wt%, both the conversion of CO and selectivity for DME decreased markedly because of the decreased activity for methanol dehydration. A mechanism for methanol dehydration to DME involving both acidic and basic sites on the HZSM-5 zeolites modified with MgO has been proposed based on the results obtained.

© 2004 Elsevier Inc. All rights reserved.

**Keywords:** Syngas; Dimethyl ether; Hybrid catalyst; Dehydration of methanol; HZSM-5 zeolite; Magnesium oxide modification

## 1. Introduction

Dimethyl ether (DME) is a useful chemical intermediate for the production of many important chemicals such as dimethyl sulfate, methyl acetate, and light olefins [1,2]. DME is also used as an aerosol propellant because of its environmentally benign properties and the belief that chlorofluorocarbons (CFCs) destroy the ozone layer of the atmosphere [3]. Moreover, DME has recently been suggested as a clean alternative fuel for diesel engines with much lower NO<sub>x</sub> emission, near-zero smoke production, and less engine noise compared with traditional diesel fuels [4].

In view of DME's potential as a clean alternative diesel fuel, much consideration should be given to the production of DME in large quantities. At present, DME is produced

in small quantities by methanol dehydration over solid acid catalysts such as  $\gamma$ -alumina and HZSM-5 zeolite, whereas methanol is synthesized from syngas over Cu–ZnO–Al<sub>2</sub>O<sub>3</sub> catalysts. However, DME will cost much more to manufacture via this process since methanol itself is an expensive chemical feedstock. Recently a method called STD (syngas to DME) was developed for the direct production of DME from syngas over a hybrid catalyst, which is composed of a methanol synthesis catalyst and a solid acid catalyst [5–7]. Compared with the conventional method, the STD process is attracting more and more industrial attention from industry because of its dramatically economic values and theoretical significance. The key steps in the STD process are supposed to be methanol synthesis, methanol dehydration, and the water gas shift (WGS) reaction [2,5,8,9]:

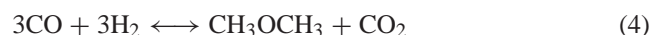


\* Corresponding author.

E-mail address: [maods@sript.com.cn](mailto:maods@sript.com.cn) (D. Mao).



The combination of reactions (1)–(3) gives the overall reaction:



since methanol formed by reaction (1) is consumed for the formation of DME and water in reaction (2). The water generated in reaction (2) is shifted by the WGS reaction (3), forming carbon dioxide and hydrogen; the latter is a reactant for the methanol synthesis in reaction (1). Thus, one of the products of each step is a reactant for another. This creates a strong driving force for the overall reaction, allowing very high syngas conversion in a single pass. For these and other reasons, the cost of production of DME by the STD process is much lower than the cost of DME production by the methanol dehydration process. For instance, according to an economic evaluation, the cost of DME production by the STD process is only about two-thirds of the cost of DME production by the methanol dehydration process [9].

Up to now, the most common hybrid catalysts reported in the literature for the STD process are the physical mixture of the methanol synthesis catalyst and the solid acid catalyst [5,6,10–13]. The Cu/ZnO-based catalyst has been used successfully for several decades for the production of methanol from syngas, and the reaction mechanism and the role of each active ingredient of the catalyst have been well studied [14–16]. In contrast to methanol synthesis, the catalytic dehydration of methanol to DME has received less attention. To date, only a few solid acids, such as  $\gamma$ -Al<sub>2</sub>O<sub>3</sub> [5,7–9], silica-alumina [8], and HZSM-5 zeolite [6,7,12,13,17–21], have been used as dehydration catalysts for DME synthesis. Among these, zeolite HZSM-5 has been used extensively because of its very high catalytic activity at the optimum reaction temperature in the syngas-to-methanol process [8,22]. However, it is well known that the strong acidic sites on HZSM-5 zeolites promote the generation of secondary products like hydrocarbons, resulting in low selectivity for DME [8,22]. Hence, the modification of HZSM-5 has become a key step in improving the selectivity for DME synthesis. The scientists at Topsøe treated the HZSM-5 zeolite with ammonia to neutralize the strong acid sites and thus inhibited the formation of hydrocarbons, but this might be expected to reduce the catalytic activity for the dehydration reaction as well. Therefore, it is necessary to develop a method to modify the zeolite HZSM-5 so that the modified catalyst catalyzes the ether formation reaction almost as well as the untreated catalyst, whereas the catalytic activity for side reactions such as the formation of hydrocarbons is eliminated.

It is well known that the acid sites in zeolites are closely related to the tetrahedral aluminum ions in the framework of the zeolite. Hence, the acidity, which is dependent on the amount of framework aluminum, can be adjusted by a proper choice of conditions of zeolite synthesis to achieve the requirements of a reaction of interest. A reasonable way to decrease the content of framework aluminum of a zeolite with an originally low Si/Al ratio obtained by hydrothermal

synthesis is offered by subsequent dealumination. Another way to reduce acidity is to introduce a further chemical compound into the zeolite system; magnesium has been used successfully in this way to improve the desired catalytic properties of zeolite HZSM-5 [23–28]. It is well illustrated in the literature [23,26] that when HZSM-5 was modified with MgO, the stronger acid sites were eliminated but the weaker acid sites increased, implying that the strong acid sites were transformed into weak acid sites. Thus it is conceivable to attempt the modification of HZSM-5 with MgO to suppress the secondary reaction of the formed DME in the STD process and at the same time to retain or decrease its catalytic activity for methanol dehydration, but to a far lesser extent. On the other hand, with this modification method we can avoid using ammonia, which is very corrosive, and ammonia is not always available in DME plants.

In this study, HZSM-5 zeolites modified with various amounts of magnesium oxide were characterized in detail and used as dehydration components of the hybrid catalysts for the direct synthesis of DME from syngas. The catalytic behavior was correlated with the structure and acidity of the modified HZSM-5; catalyst life was also examined. Moreover, a mechanism for methanol dehydration to DME involving both acidic and basic sites on MgO-modified HZSM-5 was proposed based on the results.

## 2. Experimental

### 2.1. Catalyst preparation

An HZSM-5 sample with Si/Al = 38 was prepared from original NaZSM-5 powder by repeated ion exchange with NH<sub>4</sub>NO<sub>3</sub> solutions followed by calcination in air at 550 °C. HZSM-5 modified with magnesium oxide was prepared by incipient impregnation of HZSM-5 with aqueous solutions of Mg(NO<sub>3</sub>)<sub>2</sub>, followed by drying at 110 °C overnight and then calcined at 550 °C for 3 h in an air stream.

The CuO–ZnO–Al<sub>2</sub>O<sub>3</sub> precursor (Cu:Zn:Al = 60:30:10 atomic ratio) was prepared by coprecipitation at constant pH (ca. 7) and constant temperature (70 °C). A solution containing metal nitrates ([Cu<sup>2+</sup>] + [Zn<sup>2+</sup>] + [Al<sup>3+</sup>] = 1.0 M) and a sodium carbonate solution (1.0 M) were simultaneously added to a reaction vessel containing a small amount of deionized water. All of the reagents were of analytical grade. The suspension was continuously stirred and kept at the desired pH by adjustment of the relative flow rates of the two solutions. The final suspension was aged under stirring at 70 °C for 1 h. The precipitate was filtered off and repeatedly washed with sufficient deionized water to remove residual sodium ions. The solid obtained was dried at 110 °C overnight and then calcined at 350 °C in flowing air for 6 h (catalyst).

We prepared the hybrid catalysts used for the STD reaction by physically mixing the powders (under 150 mesh) of the prepared CuO–ZnO–Al<sub>2</sub>O<sub>3</sub> catalyst and the parent

or MgO-modified HZSM-5 (2:1 wt/wt), which serve as a methanol synthesis component and a methanol dehydration component, respectively, then pressing the mixture into tablets and finally crushing them into granules (20–40 mesh) before reaction.

## 2.2. Catalyst characterization

The magnesium oxide content of the modified zeolites was determined by atom adsorption spectroscopy (AAS) on a Perkin-Elmer AA 800 instrument.

X-ray powder diffraction (XRD) measurements were performed on a Rigaku D/MAX-1400 instrument with Cu-K $\alpha$  radiation, with a scan speed of 15°/min and a scan range of 4–50° at 40 kV and 40 mA.

The surface area and pore volume of the samples were analyzed by a multipoint N<sub>2</sub> adsorption–desorption method at liquid-N<sub>2</sub> temperature (–196 °C) with a Micromeritics TriStar 3000 surface area analyzer. Samples were outgassed under vacuum to evacuate the physisorbed moisture immediately before analysis.

Acidity measurements were performed by temperature-programmed desorption of ammonia (NH<sub>3</sub>-TPD) with a conventional flow apparatus equipped with a thermal conductivity detector (TCD). A given amount of the sample, 0.1 g, was pretreated in flowing helium at 500 °C for 1 h, cooled to 150 °C, and then exposed to NH<sub>3</sub> (20 ml/min) for 30 min. The samples adsorbed by NH<sub>3</sub> were subsequently purged with He at the same temperature for 1 h to remove the physisorbed NH<sub>3</sub>. The TPD measurements were conducted in flowing He (30 ml/min) from 150 to 550 °C at a heating rate of 10 °C/min. We used CO<sub>2</sub>-TPD to examine the basicity of the modified ZSM-5 zeolites in a procedure similar to NH<sub>3</sub>-TPD.

A self-supported wafer consisting of about 10 mg of sample with a diameter of 15 mm was placed in an infrared quartz cell with CaF<sub>2</sub> windows and connected to a vacuum system. The wafer was dehydrated at 400 °C and at  $P < 10^{-6}$  mbar for 6 h. The background spectra of the samples were recorded after the self-supported wafer was cooled to room temperature and pyridine vapors were admitted to the cell. The temperature of the sample was increased to 150 °C, and the pyridine vapor was adsorbed for 5 min. Finally, excess pyridine was desorbed by evacuation of the samples at the desired temperature (150 and 350 °C) for 30 min. The samples were cooled to room temperature, and the spectra were recorded on a Bruker IFS 88 spectrometer with a resolution of 4.0 cm<sup>-1</sup>.

<sup>27</sup>Al MAS NMR spectra of the parent and modified zeolites were recorded on a Bruker AMX-400 NMR spectrometer via single-pulse experiments at a spinning speed of around 4 kHz with the use of 4-mm ZrO<sub>2</sub> rotors. Spectra were collected at a frequency of 104.26 MHz for a short pulse width of 0.5  $\mu$ s; the time interval between pulse sequences was 1 s. The <sup>27</sup>Al chemical shifts were referenced to external Al(H<sub>2</sub>O)<sub>6</sub><sup>3+</sup> in AlCl<sub>3</sub> aqueous solution. All of the

samples were equilibrated with the saturated water vapor of an NH<sub>4</sub>Cl solution before they were packed into the NMR MAS rotors.

## 2.3. Reaction studies

A pressurized flow-type reaction apparatus was used for the study. The apparatus was equipped with an electronic temperature controller for a furnace, a tubular stainless-steel reactor with an inner diameter of 6 mm, a flow regulator controller, and a back-pressure regulator. Before reaction, the hybrid catalysts (1 g) were reduced by hydrogen (5 vol% in nitrogen) in situ at 240 °C for 6 h. The syngas contained 66% H<sub>2</sub>, 30% CO, and 4% CO<sub>2</sub>. The reaction was performed under the following reaction conditions: 4 MPa, a feed rate of 1500 ml/(h g<sub>cat</sub>), and a temperature of 260 °C. The reaction products were analyzed with an on-line gas chromatograph (Hewlett-Packard 4890 D: FID detector for DME, methanol, and hydrocarbons; TCD detector for CO and CO<sub>2</sub>) after the system was stabilized for 4 h. The product lines were heated electrically to avoid unwanted condensation of the products. All gases used in this work were of high purity and were premixed into desired compositions. As measures of the catalytic activity, the conversion of CO and the selectivity of the products were used and calculated according to descriptions found in the literature [10,19].

## 3. Results

### 3.1. Characterization of MgO-modified HZSM-5

The magnesium oxide content, determined by AAS, and the surface areas and pore volumes of the parent and MgO-modified HZSM-5 zeolites are listed in Table 1. The results show that the magnesium oxide content was consistent with that added before calcination, suggesting that no noticeable loss of magnesium oxide occurred during calcination. On the other hand, both the surface areas and pore volumes decreased monotonically with an increasing content of magnesium oxide in the zeolites, which can be tentatively assigned to filling of parts of the zeolite pores with magnesium oxide.

XRD patterns of the parent and MgO-modified zeolites are compared in Fig. 1. It can be seen that with the modification with MgO the ZSM-5 structure was retained; nevertheless, the relative crystallinity decreased with increasing MgO content. In addition, no crystalline MgO was detected in the XRD spectra until the MgO content reached 10 wt%. This result is in good agreement with that reported by Wang et al. [29], who found that the dispersion capacity of MgO on HZSM-5 zeolite was 0.12 g/g<sub>HZSM-5</sub>. The above result indicates that the part of MgO that is undetectable by XRD may have been highly dispersed on the surface of HZSM-5.

NH<sub>3</sub>-TPD was performed to monitor the acid strength and the amounts of acid sites on the HZSM-5. As shown in Fig. 2, the parent HZSM-5 showed a typical NH<sub>3</sub>-TPD

Table 1  
Magnesium oxide contents and surface areas and pore volumes of the HZSM-5 zeolites

Code	MgO content (wt%)		$S_{\text{BET}}$ ( $\text{m}^2/\text{g}$ )		Pore volume ( $\text{cm}^3/\text{g}$ )	
	Nominal	Determined	Determined	Corrected <sup>a</sup>	Determined	Corrected <sup>a</sup>
HZ	–	–	331.2	331.2	0.200	0.200
MgZ1	0.5	0.50	325.1	326.7	0.198	0.199
MgZ2	1.25	1.33	311.4	315.6	0.190	0.192
MgZ3	2.5	2.65	287.4	295.2	0.166	0.170
MgZ4	5.0	4.81	249.4	262.0	0.143	0.150
MgZ5	10.0	9.62	205.5	227.4	0.125	0.138

<sup>a</sup> Corrected based on the determined content of magnesium oxide.

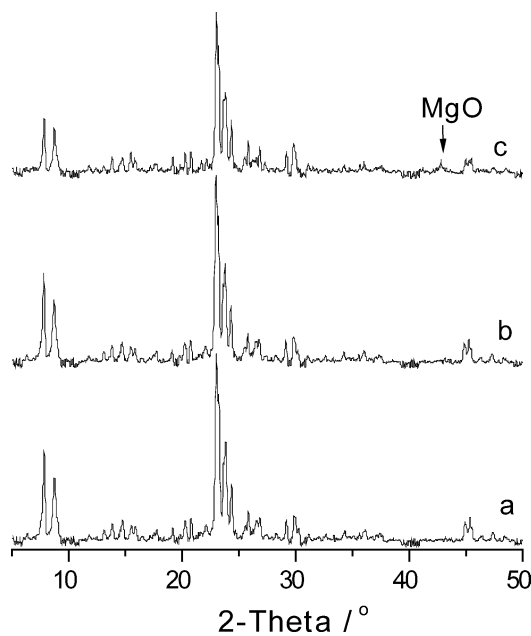


Fig. 1. XRD patterns of the parent (a) and modified ZSM-5 samples with 5 wt% (b) and 10 wt% (c) magnesium oxide.

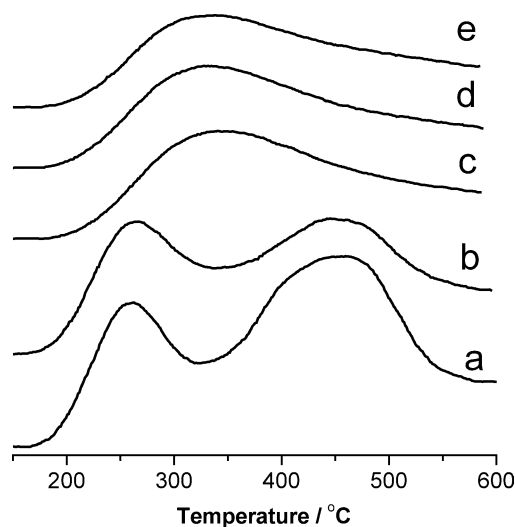


Fig. 2.  $\text{NH}_3$ -TPD profiles of the parent (a) and modified ZSM-5 samples with 0.5 wt% (b), 2.5 wt% (c), 5 wt% (d), and 10 wt% (e) magnesium oxide.

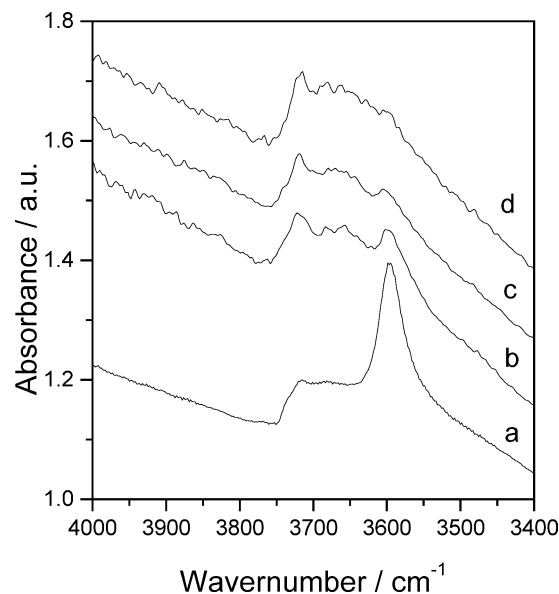


Fig. 3. Infrared spectra in the hydroxyl region of the parent (a) and modified ZSM-5 samples with 2.5 wt% (b), 5 wt% (c), and 10 wt% (d) magnesium oxide.

spectrum with two maximum peaks at 260 and 460 °C, corresponding to  $\text{NH}_3$  eluted from the weak and strong acid sites, respectively. After modification with MgO, the intensity of the high-temperature peak decreased, and that of the low-temperature peak increased slightly and shifted toward high temperatures. When the MgO content reached 2.5 wt%, only a broad peak with its maximum at 340 °C was observed. Very similar observations were also reported previously by other researchers [27,30]. At 5 wt% MgO content, the  $\text{NH}_3$ -TPD profile was almost identical to that of the 2.5 wt% MgO-modified sample. However, a further increase in MgO content to 10 wt% resulted in a decrease in the intensity of the broad peak. The results of the  $\text{NH}_3$ -TPD experiment described above show that the strength and the amounts of acid sites of HZSM-5 zeolites were effectively modified by MgO.

The IR spectra of the hydroxyl groups of the HZSM-5 zeolites before and after modification with MgO are presented in Fig. 3. The HZSM-5 sample exhibited the usual bands at 3745 and 3605  $\text{cm}^{-1}$ . The band at 3745  $\text{cm}^{-1}$  is assigned to nonacidic silanol groups, and the band at 3605  $\text{cm}^{-1}$  to acidic bridging hydroxyls [31]. The spectra of the MgO-modified zeolites had the same two major bands,



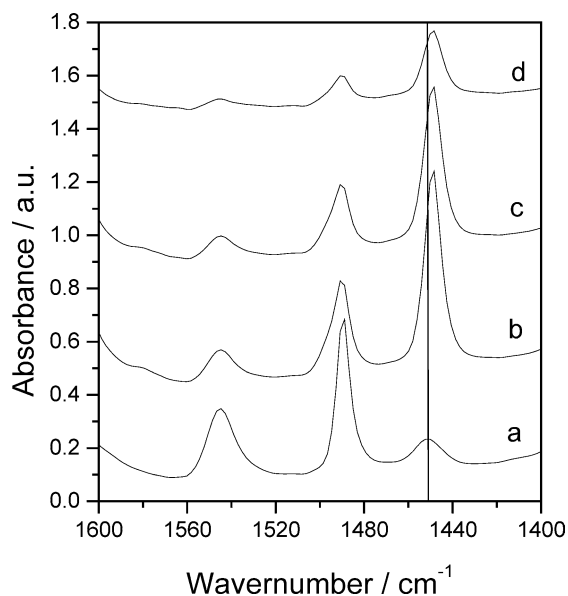


Fig. 4. FT-IR spectra of pyridine adsorbed on the parent (a) and modified ZSM-5 samples with 2.5 wt% (b), 5 wt% (c), and 10 wt% (d) magnesium oxide at 150 °C.

except that the intensity of the band at  $3605\text{ cm}^{-1}$  decreased more and more with increasing MgO content. Particularly at 10 wt% MgO loading, the bridging hydroxyl groups almost completely disappeared, whereas the intensity of the band of the silanol groups was similar to those of all other MgO-modified samples. This result indicates that the MgO strongly interacts with the acidic bridging hydroxyl groups but not with the silanol groups.

The IR spectra of pyridine adsorbed to the parent and MgO-modified zeolites are shown in Figs. 4 and 5. The spectrum of pyridine on HZSM-5 exhibited the characteristic bands at  $1543$  and  $1455\text{ cm}^{-1}$ , which are attributed to pyridinium ions (pyridine chemisorbed on Brønsted acid sites) and coordinatively bound pyridine (pyridine interacting with Lewis acid sites), respectively [32,33]. The signal at  $1490\text{ cm}^{-1}$  is assigned to pyridine on both Brønsted and Lewis acid sites. With the addition of magnesium oxide to the zeolite, the spectra changed noticeably and depended on the MgO loadings. At 2.5 wt% MgO loading, the intensities of the bands at  $1543$  and  $1490\text{ cm}^{-1}$  decreased, and that at  $1455\text{ cm}^{-1}$  increased. At the same time, the band at  $1455\text{ cm}^{-1}$  shifted to  $1450\text{ cm}^{-1}$ . (The vertical line in the figure helps to illustrate that the shift occurred.) According to the suggestion of Ward et al. [34], the new band appearing at  $1450\text{ cm}^{-1}$  can be assigned to the presence of  $\text{Mg}^{2+}$ . Therefore, the IR observations described above (Fig. 3) gave direct evidence that the substitution of  $\text{Mg}^{2+}$  for protons of hydroxyl groups, which resulted in a decrease in the number of Brønsted acid sites and an increase in the number of Lewis acid sites caused by the existence of  $\text{Mg}(\text{OH})^+$ . A further increase in MgO loading to 5 wt%, only a slight decrease in the intensity of the band at  $1543\text{ cm}^{-1}$ , and a corresponding increase in that at  $1450\text{ cm}^{-1}$  were observed.

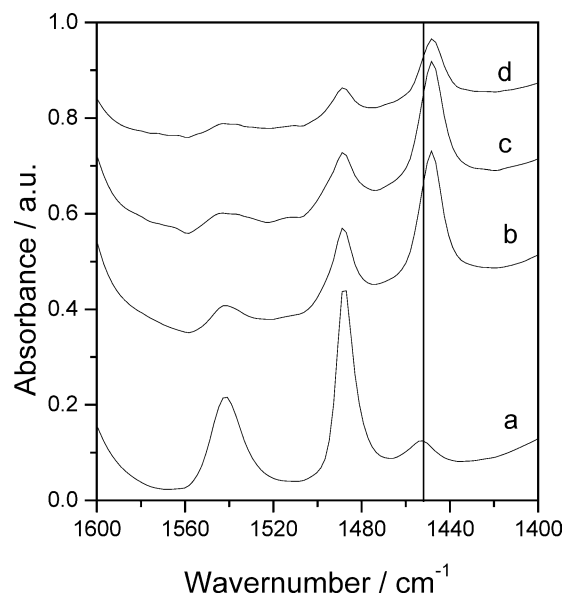


Fig. 5. FT-IR spectra of pyridine adsorbed on the parent (a) and modified ZSM-5 samples with 2.5 wt% (b), 5 wt% (c), and 10 wt% (d) magnesium oxide at 350 °C.

At 10 wt% MgO loading, the intensities of the both bands decreased significantly. This phenomenon has not been reported in previous studies, to the best of our knowledge. The above results can be interpreted as follows: when the MgO loading is lower than 10 wt%, the added  $\text{Mg}^{2+}$  reacts with the protons of bridging hydroxyls to form  $\text{Mg}(\text{OH})^+$ , so the number of Lewis acid sites increases gradually at the expense of the Brønsted acid sites with increasing MgO loading. However, when the MgO loading reaches 10 wt%, the formed  $\text{Mg}(\text{OH})^+$  groups condense with each other to form MgO ( $2\text{Mg}(\text{OH})^+ \rightarrow \text{MgO} + \text{H}_2\text{O}$ ); thus the numbers of both Brønsted-type and Lewis-type acid sites decrease. The appearance of crystalline MgO, detected by XRD, further demonstrated the proposition.

The intensities of the bands at  $1543$  and  $1455\text{ cm}^{-1}$  or  $1450\text{ cm}^{-1}$  were used to calculate the relative changes in the concentrations of acid sites after the MgO modification, which are summarized in Table 2. The data showed that modification with 2.5 wt% MgO led to a significant decrease in the concentration of the Brønsted acid sites and a remarkable increase in the concentration of the Lewis acid sites. A further increase in MgO content to 5 wt% resulted in a slight decrease in the concentration of the Brønsted acid sites and a slight increase in the concentration of the Lewis acid sites. At 10 wt% loading, the concentrations of both the Brønsted acid sites and the Lewis acid sites decreased. This result is in perfect agreement with that of  $\text{NH}_3$ -TPD. On the other hand, it is noted that for all samples investigated, the band characteristic of the bridging hydroxyl groups at  $3605\text{ cm}^{-1}$  completely disappeared after pyridine adsorption (spectra not shown here), which indicates that all bridging hydroxyl groups (strong Brønsted acid sites) were accessible for pyridine, and, therefore, a partial blocking of the pores

Table 2  
Acid sites and B/L ratios of the HZSM-5 samples modified with various contents of magnesium oxide

Sample	Brønsted acid sites ( $10^{-2}$ mg)		Lewis acid sites ( $10^{-2}$ mg)		B/L	
	150 °C	350 °C	150 °C	350 °C	150 °C	350 °C
HZ	34.53	27.18	11.19	4.46	3.08	6.09
MgZ3	12.04	5.05	53.55	25.09	0.22	0.20
MgZ4	11.20	5.93	57.78	31.70	0.19	0.19
MgZ5	4.02	2.50	20.39	12.50	0.20	0.20

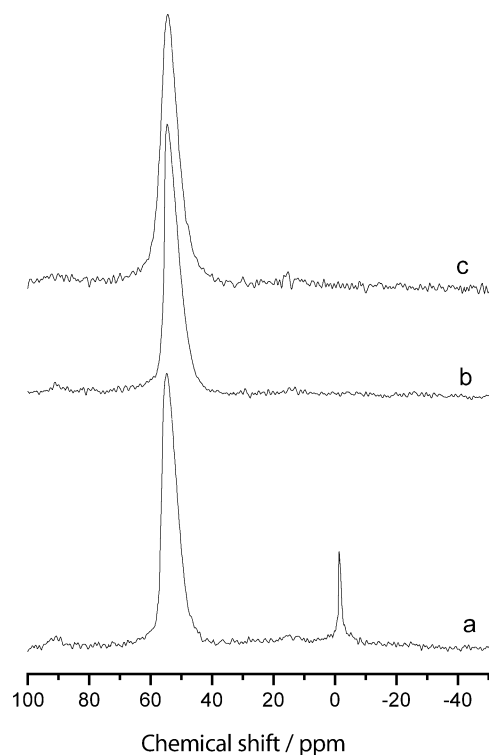


Fig. 6.  $^{27}\text{Al}$  MAS NMR spectra of the parent (a) and modified ZSM-5 samples with 2.5 wt% (b), and 10 wt% (c) magnesium oxide.

after modification of the zeolites can be excluded. Hence, it is concluded that the decrease in the surface areas and pore volumes is a result of the decrease in the crystallinity of zeolite (Fig. 1).

Additionally, Figs. 4 and 5 also showed the effect of desorption temperature on the relative intensities of the pyridine Brønsted and Lewis acid bands of the parent and MgO-modified HZSM-5 zeolites. It is evident that the relative intensities of Brønsted and Lewis acid sites decreased with increasing desorption temperature; however, the B/L ratio of the parent HZSM-5 increased and those of MgO-modified HZSM-5 zeolites remained constant with increasing pyridine desorption temperature (Table 2). Based on these results, one can conclude that the strength of the Brønsted acid sites is stronger than that of the Lewis acid sites for the parent HZSM-5 zeolite, whereas the strength of the Brønsted acid sites is equal to that of the Lewis acid sites for the MgO-modified zeolites.

$^{27}\text{Al}$  MAS NMR spectra for the parent and the modified zeolites with 2.5 and 10 wt% MgO are compared in Fig. 6.

Two peaks with chemical shifts at around 54 and 0 ppm are typically observed for HZSM-5 zeolite, which were assigned to the framework Al (FAL) and extra-framework Al oxide (EFAL) species, respectively. For both MgO-modified samples the peak at 0 ppm disappeared totally, although no effect on the framework Al was found compared with the parent material. Sun et al. [35] also reported that the small amount of extra-framework Al detected in the parent HZSM-5 was lost by Mg modification through an ion-exchange method. They thought that the loss of extra-framework Al occurred during the washing process. However, in the present work, the MgO-modified zeolites were prepared by a “dry” impregnation method without the washing process. So we conclude that the difference results from the change in the coordination environment of EFAL. A vary similar observation was also reported recently by Zheng et al. [36] for  $\text{Sb}_2\text{O}_3$ -modified HZSM-5. The above result confirms that the decrease in the concentration of the bridging hydroxyl groups after MgO modification does not result from a partial dealumination, that is, removal of Al from the T atom positions of the zeolite. In addition, the change in the coordination environment of EFAL suggests a strong interaction of MgO with EFAL.

### 3.2. Catalytic activity and stability

The hybrid catalysts with the parent and MgO-modified HZSM-5 zeolites as dehydration components were evaluated under the same reaction conditions; the results are summarized in Table 3. It can be seen that in addition to methanol and DME, relatively larger amounts of by-products like hydrocarbons (mainly lower alkanes  $\text{C}_1\text{--}\text{C}_5$ ) and  $\text{CO}_2$  were found on the catalyst with the parent HZSM-5 as its acid component. Moreover, the data in Table 3 show that methanation plays an unimportant role under the experimental conditions adopted here. A very similar phenomenon was also reported previously by other researchers [8,10]. For example, Sofianos and Scurrill [10] found that the selectivity for hydrocarbons and  $\text{CO}_2$  reached a level as high as 9.6 and 36.4%, respectively, over the admixed catalyst containing the zeolite HZSM-5 ( $\text{SiO}_2/\text{Al}_2\text{O}_3 = 90$ ) at 280 °C. However, after MgO modification of HZSM-5, especially when the content of MgO was less than 5 wt%, the formation of hydrocarbons and  $\text{CO}_2$  was decreased remarkably, so the selectivity for DME increased significantly from ca. 49% for the parent HZSM-5 to more than 64%. The strong acid sites

Table 3

Effect of modification of HZSM-5 with MgO on catalytic performance of CuO–ZnO–Al<sub>2</sub>O<sub>3</sub>/HZSM-5 for the direct synthesis of DME from syngas

MgO content (wt%)	CO conversion (C-mol%)	Selectivity (C-mol%)				Hydrocarbon distribution (C-mol%)				DME/organic products (C-mol%)
		DME	Methanol	CO <sub>2</sub>	Hydrocarbons	CH <sub>4</sub>	C <sub>2</sub>	C <sub>3</sub>	C <sub>4</sub> –C <sub>4</sub> <sup>+</sup>	
–	95.8	49.1	4.5	37.1	9.30	14.9	22.8	48.3	14.6	78.0
0.5	96.3	64.5	4.6	30.5	0.37	18.9	48.6	21.6	10.8	92.9
1.25	96.0	64.4	4.8	30.7	0.08	37.5	50.0	10.0	2.5	93.0
2.5	95.6	64.1	4.8	30.9	0.12	25.0	25.0	25.0	25.0	92.8
5.0	67.6	21.4	48.9	29.4	0.32	28.1	18.8	15.6	37.5	30.3
10.0	64.7	15.5	53.3	30.9	0.19	31.6	15.8	10.5	42.1	22.5

Reaction conditions:  $T = 260^\circ\text{C}$ ,  $P = 4\text{ MPa}$ ; H<sub>2</sub>, 66%; CO, 30%; CO<sub>2</sub>, 4%; GHSV = 1500 ml h<sup>-1</sup> g<sup>-1</sup>; CuO–ZnO–Al<sub>2</sub>O<sub>3</sub>:(MgO)HZSM-5 = 2:1 (wt/wt).

on zeolite HZSM-5 were believed to catalyze the further dehydration of the originally formed DME to lower olefins, which subsequently hydrogenize to form the corresponding paraffins [10]. At the same time, the produced water accelerated the water gas shift reaction [Eq. (3)], resulting in the formation of a larger amount of CO<sub>2</sub>. The elimination of strong acid sites of HZSM-5 through MgO modification minimized these side reactions and hence increased the selectivity for DME. Furthermore, it can be noted that the modification of HZSM-5 with MgO did not affect the conversion of CO, suggesting that the conversion of CO catalyzed by Cu–ZnO–Al<sub>2</sub>O<sub>3</sub> catalyst was the rate-determining step. On the other hand, when the content of MgO was equal to or larger than 5 wt%, the selectivity for DME decreased sharply because of the increased selectivity for methanol, which indicated that the catalytic activity for methanol dehydration had decreased noticeably. At the same time, since the methanol produced was not efficiently converted to DME, the direct synthesis of DME from syngas could not be completed, which resulted in decreased conversion of CO.

The above results suggest that, in the STD process, the conversion of CO is not dependent on the acidic property of the dehydration component, if the solid acid catalysts are so active for methanol dehydration that the intrinsic methanol synthesis rate is much lower than the methanol dehydration rate. Thus, the acidity of the solid acid catalyst affects only the selectivity for DME: the too strong acid sites promote the formation of larger amounts of by-products like hydrocarbons and CO<sub>2</sub>, resulting in lower selectivity for DME. On the other hand, when the acidity of the acidic component is not strong enough to convert effectively the originally produced methanol to DME, the acidity of the acid catalyst greatly affects both the CO conversion and the selectivity for DME: the weaker the acid sites of the acidic component, the lower the selectivity for DME and the lower the conversion of CO obtained on the hybrid catalyst. A similar conclusion had been drawn very recently by Kim et al. [13].

The stability of the hybrid catalyst with (1.25 wt%) MgO-modified HZSM-5 as a dehydration component was measured over a 100-h period, during which the reactor was operated continuously under the test conditions. The changes in the CO conversion and the selectivity for DME in organic products as a function of reaction time are depicted

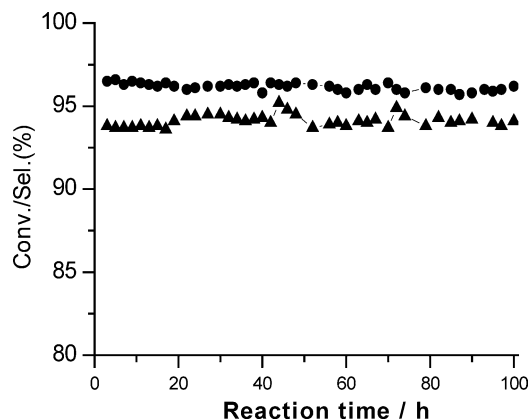


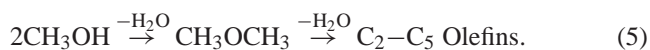
Fig. 7. Long-term test of activity and selectivity of the hybrid catalyst with HZSM-5 zeolite modified with 1.25 wt% magnesium oxide as dehydration component. (●) CO conversion, (▼) DME selectivity in organic products. Reaction conditions:  $T = 260^\circ\text{C}$ ,  $P = 4\text{ MPa}$ ; H<sub>2</sub>, 66%; CO, 30%; CO<sub>2</sub>, 4%; GHSV = 1500 ml h<sup>-1</sup> g<sup>-1</sup>.

in Fig. 7. It clearly shows that both the selectivity for DME and the conversion of CO remained essentially constant for the whole test period, which indicates that no noticeable deactivation of the catalyst is occurring.

## 4. Discussion

### 4.1. Effect of MgO modification of HZSM-5 on its catalytic activity for methanol dehydration

The dehydration of methanol to DME is a well-known acid-catalyzed reaction. However, the reaction of methanol over acid catalysts can lead to the formation of hydrocarbons such as olefins in addition to DME. The general reaction scheme given by Chang and Silvestri [37] can be outlined as follows:



The relationship between acidic properties and the catalytic performance of solid acid catalysts for methanol dehydration has been studied by many researchers. Most of them have claimed that acid sites of weak or intermediate strength are responsible for the selective formation of DME, and the strong acid sites may convert further the originally

formed DME to hydrocarbons [8,22,38,39], which makes the DME selectivity decrease. In contrast, Kim et al. [13] reported recently that the strong acid sites of HZSM-5 zeolites are responsible for the formation of DME, whereas the relatively weak acid sites appearing below 450 °C in the NH<sub>3</sub>-TPD spectra are not important for dehydration of methanol to DME. On the other hand, with respect to the nature of acid sites, Murzin and co-workers [40] proposed that the Lewis acid sites are active only for methanol dehydration to form DME, whereas strong Brønsted acid sites are required for the transformation of alcohol into hydrocarbons. Similarly, Sayed et al. [31] also reported that Lewis sites of HZSM-5 are the origin of catalytic activity in the conversion of methanol to DME, whereas dealumination Brønsted sites are the principal source of reactivity for the conversion of DME to hydrocarbons. However, Figoli et al. [38] showed that the strong Lewis acid sites on alumina also promoted the formation of hydrocarbons from alcohols.

In our cases, a comparison of NH<sub>3</sub>-TPD results and the catalytic performance of HZSM-5 before and after MgO modification leads to the conclusion that the decreased selectivity for hydrocarbons can be attributed to the decrease in the number of strong acid sites. On the other hand, although the number of strong acid sites was decreased significantly by the modification of MgO with MgO ≤ 2.5 wt%, the selectivity for methanol remained practically constant, indicating that acid sites of relatively weak strength can also efficiently convert methanol to DME. This result is inconsistent with that of Kim et al. [13] as described above. In addition, based on the pyridine adsorption IR results, it can be concluded that there is no direct relationship between the activity for methanol dehydration and the nature of acid sites on HZSM-5 zeolites. In other words, if Brønsted acid sites are the only active sites, the addition of MgO will decrease dramatically the catalytic activity for methanol dehydration. By analogy, the activity of HZSM-5 should increase with the addition of MgO if Lewis acid sites are the only active sites. Evidently, the result obtained above is at variance with that of an earlier report [31]. However, the addition of MgO greatly decreased the selectivity for hydrocarbons, suggesting that the hydrocarbons are mainly formed on strong Brønsted acid sites of HZSM-5 zeolites.

The very low activity of HZSM-5 modified with 10 wt% MgO for methanol dehydration can be realized because of its rather low acidity. But it cannot be envisaged that the HZSM-5 modified with 5 wt% MgO also exhibited very low catalytic activity for methanol dehydration, since its acidity, in both strength and nature, was almost identical to that of HZSM-5 modified with 2.5 wt% MgO. This result strongly suggests that there must be another significant factor affecting the catalytic activity for methanol dehydration besides the acidity. To identify this factor, we measured the basicities of the MgO-modified HZSM-5 zeolites with different MgO contents by CO<sub>2</sub>-TPD; the results are shown in Fig. 8. It should be noted that there are two peaks for the modified zeolites with 0.5 and 2.5 wt% MgO, one of which is

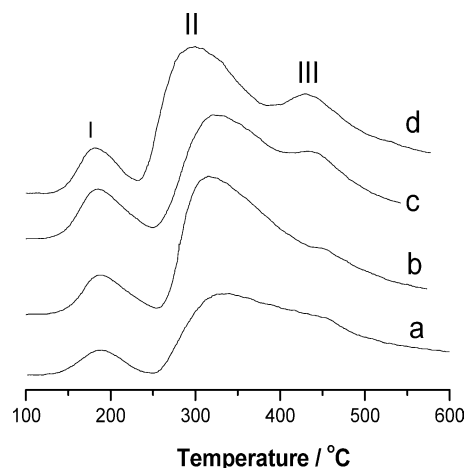
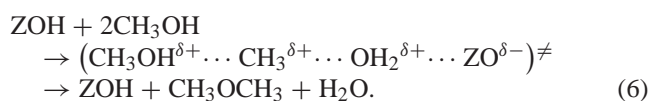


Fig. 8. CO<sub>2</sub>-TPD profiles of the modified ZSM-5 samples with 0.5 wt% (a), 2.5 wt% (b), 5 wt% (c), and 10 wt% (d) magnesium oxide.

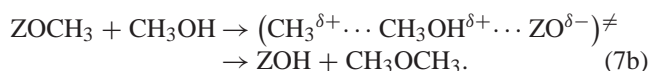
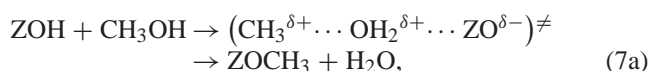
at about 180 °C (peak I) and the other is at about 330 °C (peak II). However, a new peak (III) was found on modified zeolites with 5 and 10 wt% MgO loadings (Figs. 8c and d). The peak III, at about 450 °C, represents stronger basicity than the other two peaks and should be responsible for the remarkable decrease in methanol dehydration activity on the modified zeolites with higher MgO loadings (≥ 5 wt%) than on those with lower MgO loadings (< 5 wt%).

#### 4.2. Mechanism of methanol dehydration to DME on MgO-modified HZSM-5

There are two widely considered mechanisms for the formation of DME from methanol in zeolites [41,42]. In the “direct” pathway [Eq. (6)], two methanol molecules react with each other on an acid site of the zeolite, which acts merely as a solvent. This pathway involves the simultaneous adsorption and reaction of two methanol molecules, with the formation of a DME and a water molecule in one step [43]:



Here Z stands for the zeolite framework. Alternatively, in the “indirect” pathway [Eqs. (7a) and (7b)], methanol is initially adsorbed to the zeolite. With transference of the zeolite proton the methoxonium ion is formed. This dehydrates, leaving a methyl group bonded to the zeolitic surface. Later on, those methyl groups can react with another methanol molecule to form DME [44,45]:

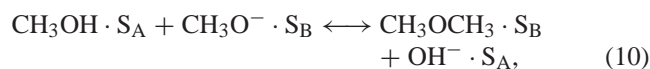
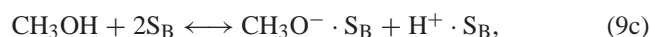


Previous theoretical studies by van Santen and co-workers [46,47] have demonstrated that the direct condensation of methanol leads to a sequence of intermediates that are lower



in energy and is therefore likely to be the preferred mechanism. In contrast, Gale and co-workers [48–50] suggested that both pathways are reasonable energetic routes. On the other hand, it should be emphasized that the reaction mechanisms involved on different zeolite type catalysts may be different. With respect to HZSM-5 zeolite used in the present work, Kubelkova et al. [51] proposed the “indirect” pathway mechanism. However, only an acidic site is required in this mechanism, which attacks the nucleophilic oxygen of the methanol molecule. Obviously, this mechanism cannot explain the catalytic results because the activities of these two modified HZSM-5 catalysts with 2.5 and 5 wt% MgO, which had acidities that were almost the same in both strength and nature, were quite different from each other.

Based on the results obtained above, the following mechanism is therefore suggested for the dehydration of methanol over MgO-modified HZSM-5 zeolites:



where  $\text{S}_A$  and  $\text{S}_B$  represent an acidic and a basic site, respectively. Eq. (9c), which is obtained by summing Eqs. (9a) and (9b), represents B-type adsorption of the methanol molecule, accompanied by dissociation into alkoxide anion and a proton. Summation of Eqs. (8)–(13) [not including (9a) and (9b)] gives the overall reaction in the heterogeneous phase:



According to the mechanism, the bimolecular reaction involves a weakly adsorbed  $\text{CH}_3\text{OH}$  on a basic site through hydrogen bonding and a strongly adsorbed  $\text{CH}_3\text{OH}$  on an acidic site through a coordination bond. It is the strongly adsorbed  $\text{CH}_3\text{OH}$  molecule on the acidic site that polarizes the C–O bond and makes the hydroxyl a better leaving group. On the other hand, the weakly adsorbed  $\text{CH}_3\text{OH}$  on the basic site enhances the nucleophilicity of the oxygen of that  $\text{CH}_3\text{OH}$  molecule. Such an alcohol molecule, considered to be an incipient alkoxide ion [52,53], can effect a nucleophilic displacement on a positively polarized carbon atom of the alcohol adsorbed to the acidic site to form ether. However, if the basicity of the basic site is too strong, the molecule adsorbed to the basic site cannot be dissociated readily into alkoxide ion and a proton [Eq. (9b)]. Thus the reaction of an alkoxide anion adsorbed to a basic site with a methanol molecule adsorbed to an acidic site cannot proceed efficiently [Eq. (10)]. Padmanabhan and Eastburn [54] also

emphasized that the interaction of methanol with the basic site should be weak. This mechanism is somewhat similar to those proposed by Padanabhan et al. [54] and Vishwanathan et al. [55] for alcohol dehydration over alumina and  $\text{TiO}_2$ – $\text{ZrO}_2$  catalysts, respectively. The mechanism suggested here can reasonably explain our experimental results.

## 5. Conclusions

Magnesium oxide can be dispersed on the surface and inside the pores of the HZSM-5 zeolite. Crystalline magnesium oxide phases were not detected until the loading of 10 wt%. A suitable amount of magnesium oxide reacted with the bridging hydroxyls to form  $\text{Mg}(\text{OH})^+$ , resulting in a decrease in Brønsted acid sites (especially the strong Brønsted acid sites) and an increase in Lewis acid sites. Hence, the selectivity for dimethyl ether increased significantly over the hybrid catalyst with the modified HZSM-5 as methanol dehydration component, because of the effective inhibition of the undesirable side reactions. These side reactions consist primarily of the further dehydration of the formed dimethyl ether to lower olefins and their subsequent hydrogenation to the corresponding paraffins; and the water gas shift reaction of CO promoted by the produced water to  $\text{CO}_2$ . However, the addition of a larger amount of magnesium oxide led to both lower dimethyl ether selectivity and lower conversion of carbon monoxide because of the lower catalytic activity for methanol dehydration. The catalytic activity of HZSM-5 zeolite modified with magnesium oxide for methanol dehydration was dependent on both the acidity and basicity. If the basicity of the catalyst is too strong, the methanol formed from carbon monoxide hydrogenation cannot be converted effectively to dimethyl ether. A mechanism for methanol dehydration involving both acidic and basic sites on HZSM-5 modified with magnesium oxide has been proposed based on the results obtained.

In summary, it is shown in this paper that the hybrid catalyst with HZSM-5 modified with a suitable amount of magnesium oxide as a dehydration component exhibits very high activity, selectivity, and stability for the direct synthesis of DME from syngas.

## Acknowledgments

We gratefully acknowledge financial support from the National Basic Research Program of China (No. 2003CB615801). The authors would like to express their sincere gratitude to those who contributed to this research: Mr. Lu Liyuan for FT-IR tests, Mr. Zhu Ming for XRD measurements, and Mr. Wang Jian for  $^{27}\text{Al}$  MAS NMR analysis. The helpful suggestions and the linguistic revision of the manuscript provided by the reviewers are also gratefully acknowledged.

## References

- [1] W.W. Kaeding, S.A. Butter, *J. Catal.* 61 (1980) 155.
- [2] G. Cai, Z. Liu, R. Shi, C. He, L. Yang, C. Sun, Y. Chang, *Appl. Catal. A* 125 (1995) 29.
- [3] T. Shikada, K. Fujimoto, M. Miyaucki, H. Tominaga, *Appl. Catal.* 7 (1983) 361.
- [4] N. Inoue, Y. Ohno, *Petrotech* 24 (2001) 319.
- [5] K. Fujimoto, K. Asami, T. Shikada, H. Tominaga, *Chem. Lett.* (1984) 2051.
- [6] J. Topp-Jorgense, US Patent 4,536,485 (1985), to Haldor Topsoe A/S, Denmark.
- [7] J.B. Hansen, F.H. Joensen, H.F.A. Topsoe, US Patent 5,189,203 (1993), to Haldor Topsoe A/S, Denmark.
- [8] T. Takeguchi, K. Yanagisawa, T. Inui, M. Inoue, *Appl. Catal. A* 192 (2000) 201.
- [9] J.L. Li, X.G. Zhang, T. Inui, *Appl. Catal. A* 147 (1996) 23.
- [10] A.C. Sofianos, M.S. Scurrrell, *Ind. Eng. Chem. Res.* 30 (1991) 2372.
- [11] K. Omata, Y. Watanabe, T. Umegaki, G. Ishiguro, M. Yamada, *Fuel* 81 (2002) 1605.
- [12] O.S. Joo, K.D. Jung, S.H. Han, *Bull. Korean Chem. Soc.* 23 (2002) 1103.
- [13] J.H. Kim, M.J. Park, S.J. Kim, O.S. Joo, K.D. Jung, *Appl. Catal. A* 264 (2004) 37.
- [14] K. Klier, *Adv. Catal.* 31 (1982) 243.
- [15] J. Nakamura, Y. Choi, T. Fujitani, *Top. Catal.* 22 (2003) 277.
- [16] X.M. Liu, G.Q. Lu, Z.F. Yan, J. Beltramini, *Ind. Eng. Chem. Res.* 42 (2003) 6518.
- [17] Q. Ge, Y. Huang, F. Qiu, *React. Kinet. Catal. Lett.* 63 (1998) 137.
- [18] Q. Ge, Y. Huang, F. Qiu, S. Li, *Appl. Catal. A* 167 (1998) 23.
- [19] Q. Ge, Y. Huang, S. Li, *Chem. Lett.* (1998) 209.
- [20] M. Jia, W. Li, H. Xu, S. Hou, C. Yu, Q. Ge, *Catal. Lett.* 84 (2002) 31.
- [21] K. Sun, W. Lu, F. Qiu, S. Liu, X. Xu, *Appl. Catal. A* 252 (2003) 243.
- [22] M. Xu, J.H. Lunsford, D.W. Goodman, A. Bhattacharyya, *Appl. Catal. A* 149 (1997) 289.
- [23] G. Cai, G. Chen, Q. Wang, Q. Xin, X. Wang, Z. Wang, X. Li, J. Liang, *Stud. Surf. Sci. Catal.* 24 (1985) 319.
- [24] J.H. Kim, S. Namba, T. Yashima, *Stud. Surf. Sci. Catal.* 46 (1989) 71.
- [25] P. Lersch, F. Bandermann, *Appl. Catal.* 75 (1991) 133.
- [26] Y. Li, W. Xie, S. Yong, *Appl. Catal. A* 150 (1997) 231.
- [27] P. Kovacheva, A. Predoeva, K. Arishtirova, S. Vassilev, *Appl. Catal. A* 223 (2002) 121.
- [28] X. Guo, J. Shen, L. Sun, C. Song, X. Wang, *Appl. Catal. A* 261 (2004) 183.
- [29] J. Wang, B.Y. Zhao, Y.C. Xie, *Acta Phys. Chim. Sin.* 17 (2001) 966.
- [30] S.Y. Li, J.W. Zhang, Z.Y. Zhou, G.Y. Cai, *Chin. J. Catal.* 10 (1989) 274.
- [31] M.B. Sayed, R.A. Kydd, R.P. Cooney, *J. Catal.* 88 (1984) 137.
- [32] N.Y. Topsoe, K. Pedersen, E.G. Derouane, *J. Catal.* 70 (1981) 41.
- [33] C.A. Emeis, *J. Catal.* 141 (1993) 347.
- [34] J.W. Ward, in: *Zeolite Chemistry and Catalysts*, in: ACS Monograph, vol. 171, Am. Chem. Society, Washington, DC, 1976, p. 118.
- [35] Y. Sun, S.M. Campbell, J.H. Lunsford, G.E. Lewis, D. Palke, L.M. Tau, *J. Catal.* 143 (1993) 32.
- [36] S. Zheng, A. Jentys, J.A. Lercher, *J. Catal.* 219 (2003) 310.
- [37] C.D. Chang, A.J. Silvestri, *J. Catal.* 47 (1977) 249.
- [38] N.S. Figoli, S.A. Hillar, J.M. Parera, *J. Catal.* 20 (1971) 230.
- [39] K.W. Jun, M.H. Jung, K.S.R. Rao, M.J. Choi, K.W. Lee, *Stud. Surf. Sci. Catal.* 114 (1998) 447.
- [40] E. Sarkadi-Priboczki, N. Kumar, T. Salmi, Z. Kovacs, D.Yu. Murzin, *Catal. Lett.* 93 (2004) 101.
- [41] J.J. Spivey, *Chem. Eng. Comm.* 110 (1991) 123.
- [42] W. Wang, M. Seiler, M. Hunger, *J. Phys. Chem. B* 105 (2001) 12553.
- [43] J. Bandiera, C. Naccache, *Appl. Catal.* 69 (1991) 139.
- [44] Y. One, T. Mori, *J. Chem. Soc., Faraday Trans.* 77 (1981) 2209.
- [45] T.R. Forester, R.F. Howe, *J. Am. Chem. Soc.* 109 (1987) 5076.
- [46] S.R. Blaszowski, R.A. van Santen, *J. Phys. Chem. B* 101 (1997) 2292.
- [47] S.R. Blaszowski, R.A. van Santen, *J. Am. Chem. Soc.* 119 (1997) 5020.
- [48] R. Shah, J.D. Gale, M.C. Payne, *J. Phys. Chem. B* 101 (1997) 4787.
- [49] E. Sandre, M.C. Payne, J.D. Gale, *Chem. Commun.* (1998) 2445.
- [50] I. Stich, K. Terakura, M.C. Payne, *J. Am. Chem. Soc.* 121 (1999) 3292.
- [51] L. Kubelková, J. Nováková, K. Nedomová, *J. Catal.* 124 (1990) 441.
- [52] H. Knozinger, K. Kochloeft, W. Meye, *J. Catal.* 28 (1973) 69.
- [53] H. Knozinger, D. Dautzenberg, *J. Catal.* 33 (1973) 142.
- [54] V.R. Padmanabhan, F.J. Eastburn, *J. Catal.* 24 (1972) 88.
- [55] V. Vishwanathan, H.S. Roh, J.W. Kim, K.W. Jun, *Catal. Lett.* 96 (2004) 23.